ACS OMEGA

Open Access

http://pubs.acs.org/journal/acsodf

Review

Graphene-Based Composite for Carbon Capture

Tri Komala Junita, Norman Syakir, Ferry Faizal, and Fitrilawati*

Cite This: *ACS Omega* 2024, 9, 20658−20669

Read Online

ACCESS | Metrics & More | Article Recommendations

ABSTRACT: The current energy system is based largely on fossil fuels that emit carbon dioxide (CO_2) and contribute to global climate change. Global energy demand is expected to increase, with growth approximately doubled by the year 2050 and tripled by the end of the century. Therefore, research and development on emissions management and carbon cycle solutions that meet energy sustainability is critical to reduce the effects of global warming. The key point of this literature review is the selection of suitable materials for carbon capture. The selection is based on the consideration that the CO_2 reduction properties are influenced by the type of material/composite that is being used, the preparation, and the possible characterization method. This Review covers graphene-based materials and their composites as appropriate materials for reducing CO_2 and their performance assessment through experiments and theoretical analysis. It is very important to improve the efficiency performance of materials and its scalability. Recently, graphene has become a widely used material for environmental applications, one of which shows good performance in reducing CO_2 concentration. To separate CO_2, graphene has been developed and is now being showcased and reviewed in this study. Given the measuring technique used, this Review is intended to be a valuable resource for individuals researching CO_2 separation employing graphene material in combination with other materials.

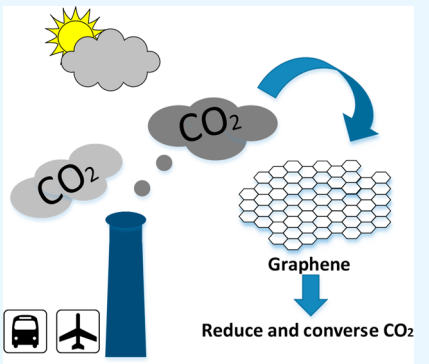

INTRODUCTION

Human activities release more carbon dioxide (CO_2) into the atmosphere than can be absorbed by natural processes. This leads to increasing levels of CO_2 in the atmosphere every year. According to NOAA's Mauna Loa Atmospheric Baseline Observatory measurements, the peak of CO_2 concentration in August 2023 was 419 ppm.[1] Fossil fuel combustion for transportation, energy production, cement production, deforestation, and agriculture are among the activities that contribute to CO_2 pollution. Those can cause CO_2 trapping in the atmosphere, prevent it from escaping into space, and result in a continuous warming of the Earth. This could trigger various weather impacts, including periods of extreme heat, droughts, forest fires, increased rainfall, floods, and tropical storm activity.[2]

The scientific design and engineering of CO_2 conversion systems has become one of the most pressing issues given the global atmosphere with increasing CO_2 concentrations and the development of conversion systems into renewable energy.[3] The quantity of anthropogenic energy-related CO_2 that helps to mitigate global climate change can be significantly reduced through carbon capture and storage (CCS). Therefore, picking a quality raw material is crucial for implementing this technology. As shown in Figure 1, CO_2 has the perfect adsorbent characteristics. Adsorbent substances should typically be highly selectable, have high adsorption capacities, be long-lasting, etc.[4]

There are several methods used to capture CO_2 such as adsorption,[5] membrane separation,[6] absorption,[7] cryogenic distillation,[8] and chemical looping combustion.[9] CO_2 can be converted into nontoxic chemicals to reduce emissions and meet energy needs. Some of the methods used for CO_2 conversion are electrochemical,[10] catalytic,[11] and photocatalytic.[12−14] Photocatalysis is a highly effective method for converting CO_2 into valuable chemicals, including methane, methanol, formaldehyde, ethanol, and hydrocarbons, which have been identified.[15] To cater demands of large-scale industrial applications, chemical costs and energy consumption must be minimized to the fullest extent possible.[16] Various adsorbent materials that have been developed recently are zeolite,[17] metal oxides,[18] porous polymers,[19] metal−organic frameworks (MOFs),[20] porous silica,[21] and carbon materials.[22]

Graphene is a remarkable material with high conductivity, tensile strength, and surface area, making it useful for a wide range of applications. However, graphene tends to aggregate, creating hydrophobic regions, so it is oxidized to produce graphene oxide (GO) to reduce its conductivity and $\pi-\pi$ buildup. GO is highly functional and can be dispersed in water

Received: November 3, 2023
Revised: April 8, 2024
Accepted: April 12, 2024
Published: April 30, 2024

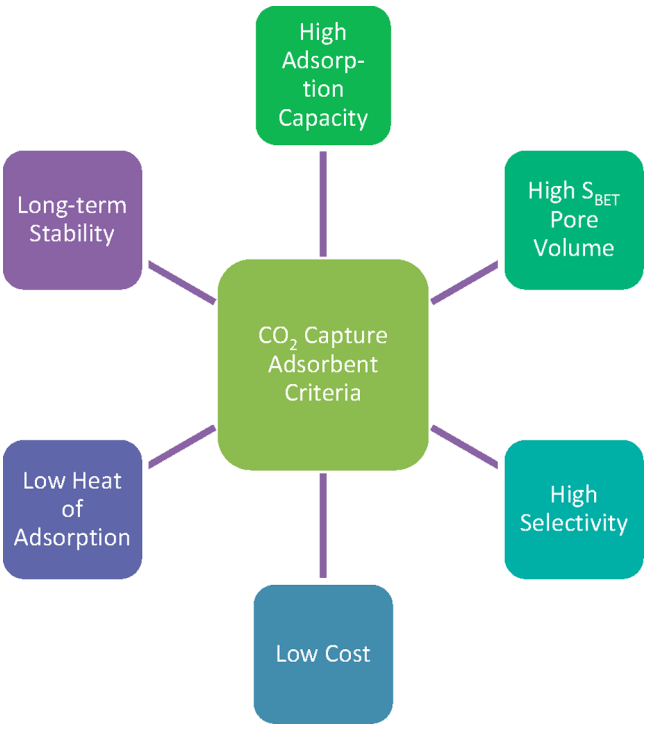

Figure 1. Standards for an optimal adsorbent for CO_2 capture. Adapt with permission from ref 4. Copyright 2021 Elsevier.

and organic solvents. Reduction of GO can improve its electrical conductivity, leading to the formation of reduced graphene oxide (rGO).[23]

The popularity of graphene-based materials stems from their unique physical, chemical, structural, and morphological characteristics, as well as their flexibility in processing and functionalization. They are compatible with organic solvents, have exceptional mechanical properties, and exhibit superior resistance to aggressive acidic or alkaline conditions. Scientists are extensively studying these materials for their potential applications in various fields, including energy,[24] sensing,[25] water treatment,[26] electronics,[27] and material reinforcement.[28] For CO_2 separation applications, researchers are looking into various graphene-based configurations, including laminated graphene, nanoporous graphene, and graphene-based composites. For instance, CO_2 can be effectively separated from a variety of CO_2 mixtures, including CO_2/O_2, CO_2/CH_4, CO_2/N_2, and CO_2/H_2, using nanoporous graphene made from other forms of carbon or through the reduction of GO.[29]

The chemical reduction of GO is a highly successful and reliable method for producing nanosheets of rGO on a large scale and at a low cost. With the added advantage of chemical modification of the rGO surface, this technique enables the formation of composites with various materials. As shown by extensive research in this field, graphene-based composites' distinctive electronic and optical characteristics make them highly desirable for a variety of potential applications.[30]

Review articles for CO_2 reduction should be published more frequently. Previously there had been a journal review that used amine-functionalized materials for CO_2 capture.[31] However, amine materials are not environmentally friendly so environmentally safe materials are still being studied. An overview of the characteristics and difficulties of graphene and GO-based membranes for gas separation was given by Yoo et al. in 2017,[32] while in 2020, Khandaker et al.[33] investigated carbon nanomaterials, mesoporous materials, biochar and activated biochar, and activated carbons for CO_2 capture. Singh et al.[29] also reported a review in 2021 on gas separation with graphene-based membranes. However, after examining these reports, which primarily focused on gas separation in general, a comprehensive review of CO_2 reduction by graphene is urgently needed, given the rapidly evolving field of carbon capture.

This article will review 15 journals[34−48] on the performance of graphene composite with other materials for carbon capture. The methods of CO_2 capture that will be reviewed in this systematic review are adsorption, photocatalytic, and membrane separation. Adsorption uses adsorbents to reduce CO_2, membrane separation uses polymers to filter CO_2, and photocatalysis uses light energy to reduce and convert CO_2 to fuel cells. Each journal discusses graphene synthesis approaches, CO_2 measurements, and its performance in reducing CO_2.

METHODS

This Review aims to determine the performance of graphene-based composites in reducing CO_2. The selection of a suitable material can initiate a promising carbon capture technology. It can be used to solve environmental problems. The systematic review refers to a PRISMA 2020 flow diagram[49] consisting of three steps to achieve this goal: identification, screening, and included, as shown in Figure 2.

The first step was to identify the database. Searches were carried out on ScienceDirect, Scopus, and Springer by entering keywords that are the topics of the research to be reviewed.

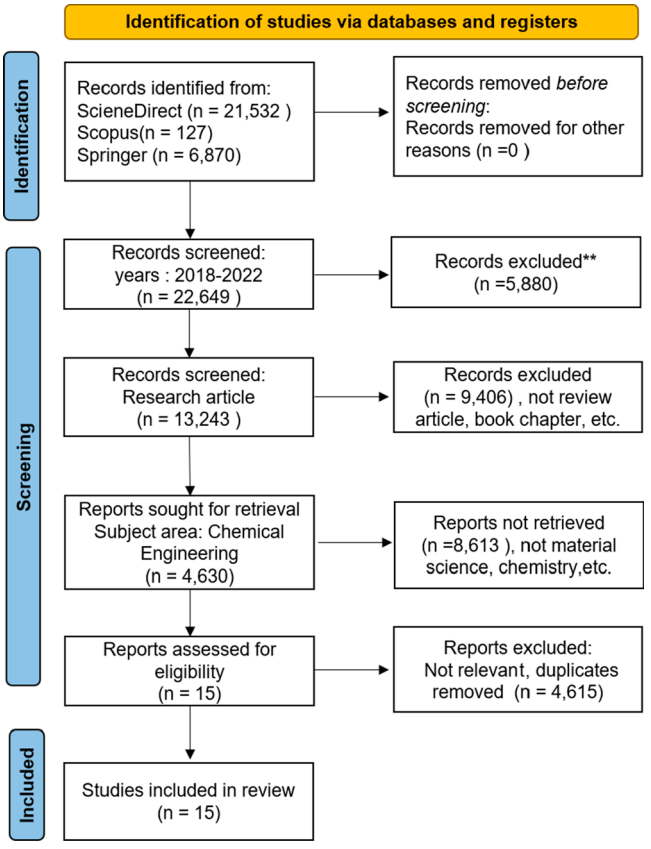

Figure 2. PRISMA 2020 flow diagram for systematic reviews. Adapt with permission from ref 49. Copyright 2021 Elsevier.

https://doi.org/10.1021/acsomega.3c08722
ACS Omega 2024, 9, 20658−20669

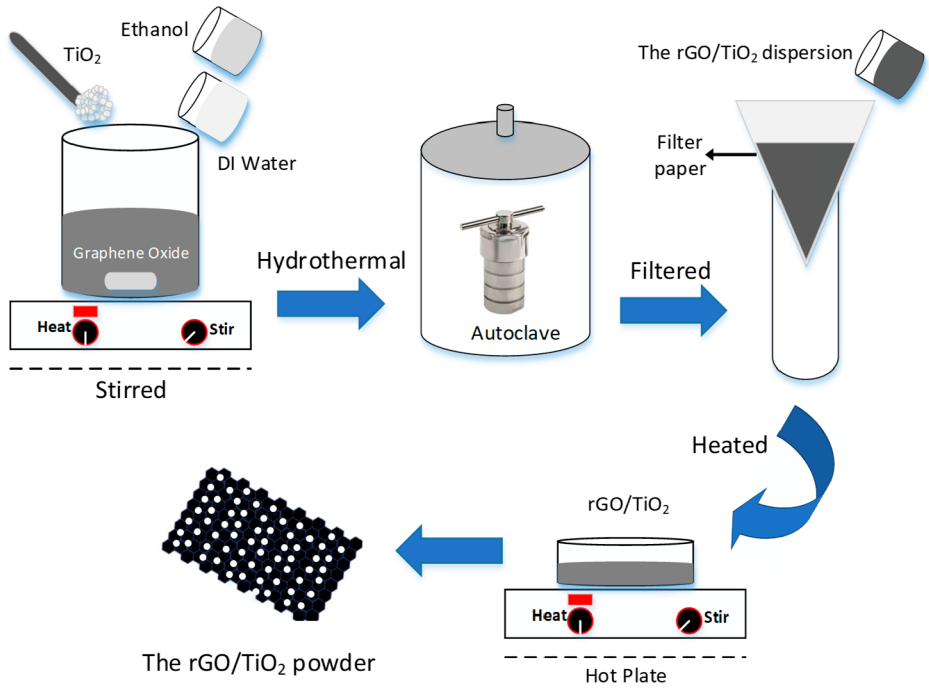

Figure 3. Synthesis of a graphene-based composite with TiO_2 using a hydrothermal method.

Some keywords were determined from research objectives. Keywords consisting of graphene composites (including GO, reduced GO, etc.) and carbon capture were entered into the search process.

From this search, 28 529 documents were found, namely 21 532 on ScienceDirect, 127 on Scopus, and 6870 on Springer, which then proceeded to the screening stage.

In this section, the total number of identified documents was used to determine the year of publication. In each search, the years of publication were restricted to 2018−2022. As a result, there were 17 194 documents from ScienceDirect, 82 documents from Scopus, and 5373 documents from particular Springers. The remaining documents were then filtered by paper type to include only research papers. There were 9939 ScienceDirect articles, 71 articles on Scopus, and 3233 articles on Springer when filtering only "research articles" was taken into account. Since there are still many selected article candidates, the screening process was carried out by selecting the subject area Chemical Engineering, which is related to the topic to be reviewed. Chemical engineering focuses on developing efficient and sustainable chemical processes to reduce CO_2 emissions. This can involve gas separation technologies, catalysis, and the development of environmentally friendly reactors.

Using that screening process, 3169 documents from ScienceDirect, 29 from Scopus, and 1432 from Springer were found. Then, checking the title and abstract was the next step in screening. For full-text analysis, the title and abstract were included if they contain one or more keywords or search terms. As a result, this step removed 4532 articles and left only 98 articles. Out of the 98 articles, only 15 articles were selected because there were several duplicate articles, and several articles needed to be selected considering the results of their research, making it difficult to review with other articles.

After thorough text analysis, there were 15 articles chosen for this investigation. The outcomes of materials composited with graphene to reduce CO_2 are described in these articles. Besides being influenced by the material, the results are also affected by temperature, pressure, and humidity during the experimental process.

SYNTHESIS OF GRAPHENE

This research uses graphene-based composites. Graphene consists of derivatives such as graphene oxide (GO), reduced graphene oxide (rGO), and graphene modified with various materials.

Several journals reported GO prepared by using the Hummer method. F. E. Che Othman et al.[45] synthesized graphene oxide using Hummer's method. In that work, graphite powder and $NaNO_3$ were mixed with concentrated H_2SO_4 and stirred at <20 °C. Then, $KMnO_4$ was added, stirring the mixture for 30 min before quenching with DI water. Furthermore, the solution was heated to 98 °C and stirred overnight. After that, H_2O_2 and a HCl solution (5%) were added to eliminate metal ions. The substance was washed, filtered, and dried under a vacuum to obtain GO. The rGO was obtained through thermal reduction and exfoliation of GO at >800 °C. Several studies have also reported rGO synthesized by various methods, namely solvothermal[37] and hydrothermal,[41] as shown in Figure 3.

In another study, W. Ren et al.[46] used graphene aerogel (GA) as a composite base material. After mixing GO dispersion with L-ascorbic acid at 95 °C for 25 min, partially reduced graphene hydrogel (GH) was created. GH was frozen, melted, and left to concentrate for 10 min. After washing with ethanol, GH was dried at 60 °C for 12 h to produce GA. GO was modified by Y. Zhao et al.[34] by adding L-arginine, resulting in GO-Arg (GO-L-arginine). The synthesis of GO-Arg involved mixing 0.2 g of GO powder and 6 mmol of L-arginine dissolved in 60 mL of NaOH and stirring for 12 h, with the suspension fully reacting to form a sodium arginate solution. The end product was obtained as black solid particles through centrifugation and referred to as GO-Arg. R. Casadei et al.[43] synthesized porous graphene oxide (PGO). To prepare

https://doi.org/10.1021/acsomega.3c08722
ACS Omega 2024, 9, 20658−20669

PGO, 2 mg/mL of GO dispersion was sonicated for 30 min, and NH_4OH and H_2O_2 were added in a 20:1:1 ratio at 50 °C. Then it was stirred for 5 h and centrifuged at 12 000 rpm for 1 h. Furthermore, the mixture was redissolve in DI water and dialyzed for 3−4 days while monitoring the pH until it reached 7.

Other studies have also reported modified GO without adding other materials. A. M. Varghese et al.[47] made UV-GO by exposing GO to a UV light for varying amounts of time with an intensity of 0.76 W/m^2 at 40 °C. H. Kweon et al.[48] synthesized two types of graphite oxides (GOs): partially oxidized GO (P-GO) and highly oxidized GO (H-GO). Preoxidation of H-GO was performed before it underwent a further 4 days oxidation process using a 1:6 mass ratio of graphite to oxidant. The 460 mL of concentrated H_2SO_4, 60 g of $KMnO_4$, and 10 g of graphite were combined to create P-GO. Both samples were washed with a 1:10 HCl solution, filtered, and dried at either room temperature or 80 °C to remove any remaining metal ions. To get rid of metal ions and acid, the GO products were dialyzed.

VARIOUS METHODS FOR CARBON CAPTURE

To properly evaluate the viability of graphene composites for carbon capture, a thorough analysis of various measurements must be conducted. This analysis should include a comparative performance assessment of critical factors such as adsorption, gas permeation, and photocatalytic reduction.

Adsorption. Adsorption methods in CO_2 capture have an advantage. This method is widely studied for its broad operating range, low energy consumption, and ease of implementation.[37,38] The problem is although a CO_2 adsorbent is both efficient and stable, it is important to note that adsorption only works until the adsorbent reaches a saturation. In the adsorption method, CO_2 attached to the porous surface of the adsorbent will be adsorbed to reduce CO_2, as shown in Figure 4. To prevent the graphene-based adsorbent from saturation, graphene is composited with other materials to increase its absorption capacity.

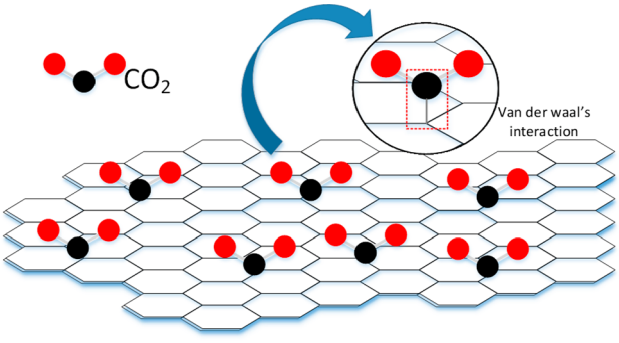

Figure 4. Mechanism of CO_2 adsorption by graphene-based composite.

Several studies have used adsorption methods for carbon capture as in the experiments utilizing a homemade breakthrough curve, as in Table 1. Y. Zhao et al.[34] analyzed a CO_2 adsorption using gas-by-gas chromatography (GC9790II). Experiments were conducted in the study at three different temperatures (25, 50, and 70 °C) and flow rates (40, 60, and 80 mL/min). Additionally, based on the ideal temperature and gas flow rate for each sample, the CO_2 adsorption capabilities

Table 1. Adsorption Data of CO_2 Separation from Graphene-Based Composite

graphene composites	CO_2 uptake (mmol/g)	pressure (bar)	temperature (°C)	ref
MOF/GO-Arg	3.371		50	34
PpPDA/rGO(APG-1%)	4.65	5	25	40
rGO/NPC-600-2-1	5.77		25	41
rGO/ACNF0.1	58	15	25	45
CuBTC/GA-IL	3.71	1		46
LDH/GO01	4.51			36
GO(0.25)/MR-500	5.21			44
HKUST-1@10UV-GO	9.50	1	0	47

of the samples were assessed under three different humidities (15, 45, and 55%). In order to determine how humidity would affect the gas flow, water vapor was added. One gram of adsorbent was put into each sample column. All synthetic MOF samples were subjected to breakthrough measurements to examine the dynamic CO_2 adsorption capacity using a binary gas mixture that contained 15% CO_2 and 85% N_2, which was representative of the industrial flue gas streams from power plants at ambient temperature and pressure.

MOF/GO-Arg had the highest CO_2 adsorption capacity at 50 °C, with a saturation capacity of 3.371 mmol/g. The order of adsorption capacities was MOF/GO-Arg > MOF/GO > Cu-BTC (also known as HKUST-1 or MOF-199). Lower flow rates resulted in longer contact time and higher adsorption capacity. At higher flow rates, the adsorption amounts decreased and breakthrough times shortened. Comparing the three adsorbents' CO_2 adsorption performances, all three had faster breakthroughs under 55% humidity than other levels. The fastest breakthrough was achieved by Cu-BTC and the slowest by MOF/GO-Arg. Small amounts of water encourage CO_2 adsorption, but large amounts of water vapor reduce effectiveness. CO_2 adsorption decreased from 3.371 to 2.511 mmol/g at 55% humidity.[34]

Y. Wang et al.[40] tested how much CO_2 can be absorbed by specific samples at different pressures and temperatures in a setup as shown in Figure 5. They used nitrogen-doped polyphenylene/GO composites to N-doped activated carbon (APG). They found that all samples had a high capacity for CO_2 at low pressure due to chemical adsorption, but the

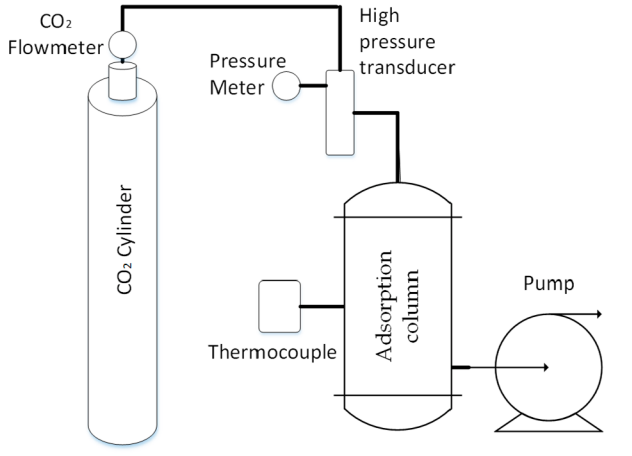

Figure 5. Setup for adsorption of CO_2.

https://doi.org/10.1021/acsomega.3c08722
ACS Omega 2024, 9, 20658−20669

increase slowed at higher pressure, likely due to physical adsorption. Specifically, at a temperature of 298.15 K and pressure of 5 bar, APG-1% (1% represents GO mass ratio) shows the best performance with a CO_2 capacity of 4.65 mmol/g. Moreover, it is essential to note that various pyrolysis temperatures and KOH additions were tested. It is worth mentioning that APG-1%-600-0 (1% represents GO mass ratio, 600 represents pyrolysis temperature (°C), and 0 represents KOH mass ratio) without an activator exhibits a meager CO_2 adsorption capacity of 1.71 mmol/g, with a surface area of only 235.7 m^2/g. However, an excessive amount of KOH (APG-1%-600- 4) in the pyrolysis process may lead to the destruction of micropores and the formation of a macropore structure (pore size = 74.3 nm), resulting in reduced surface area and pore volumes. Besides, the pyrolysis temperature is a crucial factor affecting the degree of activation. It is observed that a large surface area is related to a high CO_2 adsorption capacity, and the appropriate temperature and KOH amount lead to a larger surface area. Nevertheless, APG-1.5% (1011.9 m^2/g) and APG-1%-600-2 (1059.7 m^2/g) have relatively low capacities of 3.94 and 3.95 mmol/g, respectively. The reason for this can be traced back to the overreaction which has resulted in a relatively low N content.[40]

J. Xiao et al.[41] used rGO/N-porous carbon to examine the static CO_2 adsorption of all samples at 298 K under 500 KPa. It was found that raising the activation temperature from 400 to 600 °C significantly improved the activated samples' CO_2 adsorption capabilities. When the activation temperature was raised to 700 °C, there was a slight decrease, though. This trend continued as the mass ratio of KOH activator and GO addition was increased. In general, it can be said that under the same circumstances, a material's porous structure and chemical properties are closely related to its ability to absorb CO_2.

The maximum adsorption capacity of rGO/NPC-600-2-1 (600 for activation temperature at 600 °C, 1 indicates the amount of graphene oxide addition at 1% of the total mass of glucose and dicyandiamide, 2 indicates the mass ratio of potassium hydroxide to carbon composite material precursor) was 5.77 mmol/g[41], it should be noted. A control sample, rGO/PC-600-2-1, was prepared and used without N doping to evaluate the effect of N heteroatoms on increasing CO_2 adsorption capacity.

When compared to the rGO/NPC-600-2-1 sample under identical adsorption conditions, the nitrogen-free rGO/PC-600-2-1 sample's CO_2 adsorption capacity at 298 K and 500 kPa was significantly lower at 2.0756 mmol/g. According to the data, the rGO/NPC sample's ability to adsorb CO_2 is directly correlated with the heteroatom N's presence.[41]

To analyze the sample's adsorption isotherm, they utilized three models: Langmuir, Redlich−Peterson, and Freundlich. To study how temperature affects the efficiency of CO_2 adsorption for rGO/NPC-600-2-1, they also experimented at 323 K. For rGO/NPC-600-2-1, the maximum CO_2 equilibrium adsorption rates were 5.77 mmol/g at 298 K, 4.98 mmol/g at 308 K, and 4.24 mmol/g at 323 K. The exothermic nature of CO_2 adsorption on rGO/NPC-600-2-1 is noteworthy, and lowering the adsorption temperature can increase the rate of adsorption.[41]

In their study, L. Ouyang et al.[44] determined the static equilibrium adsorption capacity of CO_2 at 298.15 K (100/500 kPa). They used melamine−resorcinol−formaldehyde resin composited with graphene oxide (MR/GO). All samples' adsorption capacities were found to increase as pressure was raised. GO (0.25)/MR-500 (0.25 is the amount of GO used in weight %, and 500 indicates the activation temperature of 500 °C) demonstrated the best CO_2 adsorption performance of the samples, with a capacity of over 2.27/5.21 mmol/g. However, it was discovered that GO (0.25)/MR without activation had absolutely no capacity for CO_2 adsorption. Additionally, the CO_2 adsorption capacities of GO (0.25)/MR-600 and GO (0.25)/MR-700 decreased to 1.33/4.29 and 0.87/1.89 mmol/g at 100/500 kPa, respectively, as the activation temperature rose from 500 to 600 and 700 °C. The CO_2 adsorption capacities of MR-500 without GO and GO (0.375)/MR-500 were 0.19/0.49 and 0.74/2 mmol/g , respectively. This trend, which was discovered to be consistent with the samples' surface area and micropore volume, suggests that the CO_2 adsorption capacity may be improved with an increase in surface area and micropore volume.

GO (0.25)/MR-500 displays fast kinetics of CO_2 adsorption, reaching 90% within 2 min and 97% within 10 min. For CO_2, the calculated equilibrium absorption capacity is 4.87 mmol/g, and the diffusion time constant is 2.11 min^{-1}. GO (0.25)/MR-500 is highly advantageous for reducing the adsorption cycle time in potential practical applications due to its quick kinetics. In addition to rapid adsorption kinetics, an adsorbent's CO_2/N_2 selectivity for CO_2 capture is also crucial. GO (0.25)/MR-500 exhibits a deficient N_2 adsorption capacity of 0.492 mmol/g (298.15 K and 500 kPa). The highest CO_2/N_2 selectivity of 58 is reached at 20 kPa, gradually decreasing to 39 at 100 kPa and 19 at 500 kPa. This selectivity level for high-pressure CO_2 adsorption is still significantly high compared to the previously reported porous carbons. For highly selective CO_2 adsorption at low pressure, surface-doped N, especially pyrrolic-N, offers a wealth of sites. Adsorption was done at 298.15 K and high pressure (500 kPa), and in situ regeneration was done at 373 K and in a vacuum to evaluate the stability and recyclability of GO (0.25)/MR-500 in CO_2 adsorption. After five adsorption−desorption cycles, GO (0.25)/MR-500 continues to exhibit exceptional stability, holding onto its 4.66 mmol/g CO_2 adsorption capacity and 98.5% recovery rate.[44]

In the study by Y. Yang et al.,[36] they utilized Shimadzu automatic differential thermogravimetry (TGA, DTG-60H) to evaluate the CO_2 adsorption performance of GO in LDH (layered double hydroxide)/GO composites. The LDH/GO composites loaded with various amounts of alkali metal nitrates ($(Li_{0.3}Na_{0.18}K_{0.52})NO_3^-$) had their ability to capture CO_2 captured and evaluated. LDH/$GO_{0.5}$'s CO_2 uptake at *m*LDH:*m*GO = 10:0.5 with $(Li_{0.3}Na_{0.18}K_{0.52})NO_3^-$ was only 0.35 mmol/g. The CO_2 uptake initially decreased as the amount of $(Li_{0.3}Na_{0.18}K_{0.52})NO_3^-$ loading increased. The capacity of LDH/$GO_{0.5}$ to adsorb CO_2 increased from 0.35 to 3.13 mmol/g when the loading amount of $(Li_{0.3}Na_{0.18}K_{0.52})$-$NO_3^-$ was raised from 10 to 30 mol %. However, when the amount of $(Li_{0.3}Na_{0.18}K_{0.52})NO_3^-$ that was loaded was increased further to 40 and 50 mol %, respectively, the CO_2 uptake fell to 2.74 and 1.71 mmol/g. The CO_2 uptake was 0.52 mmol/g among samples of pure LDH/$GO_{0.7}$ at *m*LDH:*m*GO = 10:0.7. The CO_2 uptake was 0.52 mmol/g among samples of pure LDH/$GO_{0.7}$ at *m*LDH:*m*GO = 10:0.7. The capacity to capture CO_2 showed a pattern of rising and then falling as the $(Li_{0.3}Na_{0.18}K_{0.52})NO_3^-$ loading amount gradually increased. LDH/$GO_{0.7}$'s CO_2 uptake increased from 1.01 to 4.3 mmol/g when the amount of $(Li_{0.3}Na_{0.18}K_{0.52})NO_3^-$ loading was increased from 10 to 30 mol %. LDH/$GO_{0,7}$'s ability to

https://doi.org/10.1021/acsomega.3c08722
ACS Omega 2024, 9, 20658−20669

absorb CO_2 decreased to 3.74 and 1.44 mmol/g, respectively, as the loading capacity of $(Li_{0.3}Na_{0.18}K_{0.52})NO_3^-$ was further increased to 40 and 50 mol %. LDH/GO_1 can absorb up to 0.77 mmol/g of CO_2. The increase in LDH/GO_1's CO_2 uptake from 2.58 to 4.51 mmol/g occurred when the loading amount of $(Li_{0.3}Na_{0.18}K_{0.52})NO_3^-$ was increased from 10 to 30 mol %. However, when it was increased to 40 and 50 mol %, respectively, the LDH/GO_1 CO_2 sorption amount decreased to 3.27 and 2.07 mmol/g.[36]

On a rig, static volumetric CO_2 adsorption measurements were reported by F. E. Che Othman et al.[45] Prior to CO_2 adsorption, the sample (0.5 g) was vacuum-dried for 12 h at 150 °C to remove moisture. For each test, the activated carbon nanofibers (ACNFs) and CO_2 were loaded into the adsorption cell (AC) and loading cell (LC) until the desired pressures of 5, 10, and 15 bar, respectively, were reached. The gas adsorption test was initiated as soon as the required pressure was reached, and CO_2 (adsorbates) and ACNFs (adsorbents) were introduced in the AC by turning the valve between the AC and LC. To determine the pristine and composite ACNFs' adsorption capacities at low and moderate pressures, these three pressures were used. Every 5 min until the pressure reached equilibrium, the temperature in the AC and LC as well as the pressure was recorded. When the temperature and pressure remained constant for roughly 10 min, adsorption equilibrium was reached. At room temperature and various adsorption pressures, the CO_2 adsorption performance of pure ACNF and composite was examined as a function of time until equilibrium was reached. At a pressure of 5 bar, rGO/$ACNF_{0.1}$ (0.1 for the amount of rGO indicating 10% weight of rGO) displayed the highest CO_2 uptake among other composites, almost doubling the uptake value of ACNF (41 vs 24 mmol/g).[45]

All samples had consistent trends at all pressures. The fact that CO_2 uptake increased as adsorption pressure increased suggests that the process of CO_2 capture by this kind of adsorbent is known as physisorption. Even though a moderate SBET was obtained, it is interesting to note that the CO_2 uptake of rGO/$ACNF_{0.1}$ increased, making it a potentially excellent future CO_2 adsorbent with relatively higher adsorption values compared to previously discovered CO_2 adsorbent materials.

The N_2 and CO_2 adsorption isotherms of all samples were measured by W. Ren et al.[46] using a Quantachrome Autosorb-iQ2 sorption analyzer at 298 K. To investigate the dynamic adsorption performance of the adsorbents, breakthrough experiments were conducted in a fixed adsorption bed. The CO_2 adsorption isotherms reveal that CO_2 uptake of graphene aerogel (GA) was significantly lower than that of CuBTC (also known as HKUST-1 or MOF-199) by 0.34 and 3.01 mmol/g, respectively. Due to the high pore volume of composites, adding CuBTC to GA slightly improves its ability to absorb CO_2 (CuBTC/GA, 3.26 mmol/g). The low pore volume of CuBTC/GA-IL (ionic liquid) causes its CO_2 uptake to be less than that of CuBTC-IL. However, CuBTC/GA-IL's CO_2 uptake is still greater than CuBTC/GA's (3.71 vs 3.26 mmol/g), emphasizing the significance of IL addition in enhancing CO_2 adsorption capability. The CO_2 uptakes of CuBTC-IL and CuBTC/GA-IL are significantly higher than their N_2 uptakes, indicating their outstanding CO_2/N_2 performance, according to the experiment's N_2 and CO_2 adsorption isotherms. The Ideal Adsorbed Solution Theory (IAST) model predicted that the CO_2/N_2 selectivity of CuBTC/GA-IL decreases with increasing pressure. This model was based on the CO_2 and N_2 adsorption isotherms of GA, CuBTC-IL, and CuBTC/GA-IL in a CO_2/N_2 mixture (20/80% v/v). CuBTC/GA-IL has slightly better CO_2/N_2 selectivity at low pressure but is almost identical with CuBTC-IL at 1 bar. CuBTC/GA-IL's hierarchical pores make it more favorable due to faster mass transfer, so both were used in subsequent experiments.[46]

A. M. Varghese et al.[47] conducted CO_2 adsorption performance tests using a Micromeritics 3Flex Analyzer in static volumetric mode. The adsorbent within the analyzer was subjected to various humidity levels. They used UV-GO and GO to measure the CO_2 adsorption isotherms of the pure HKUST-1 and HKUST-1 hybrids at 25 °C and up to 1 bar of pressure. Notably, the capacity of HKUST-1@GO was lower than that of HKUST-1, whereas the capacities of both HKUST-1@UV-GO hybrids were higher. The HKUST-1 hybrid with 10UV (10-h UV treatment)-GO demonstrated a notable 45% (5.14 mmol/g) increase in capacity. At various temperatures, they also measured CO_2 adsorption isotherms up to 1 bar. At temperatures of 0, 25, 40, and 60 °C, the 10UV-GO MOF hybrid showed an increase in CO_2 uptake of 30%, 45%, 49%, and 55% in comparison to the pure MOF. The capacities at 0 °C were higher when comparing the adsorption performance at various temperatures (9.5, 7.6, and 7.3 mmol/g for the respective 10UV-GO MOF hybrid, 1UV-GO MOF hybrid, and neat HKUST-1), indicating that lower temperatures favor physisorption, which dominates the adsorption mechanism. The lack of strong binding causes the adsorbate molecules to become more mobile and more likely to move away from the surface at higher temperatures rather than sticking to it. In this study, the HKUST-1@10UV-GO adsorbent's capacity at 0 °C and 1 bar was 9.5 mmol/g, the highest of all the tested materials and conditions.[47]

Membrane Separation. A membrane is an indispensable selective barrier that features pores, an ideal attribute for isolating molecules or ions from a mixture. The mechanism of CO_2 separation using membrane separation is shown in Figure 6. Permeability and selectivity are the primary features determining a membrane's effectiveness. Selectivity is the permeability ratio of more permeable components to less permeable ones, whereas permeability refers to a substance's capacity to pass through a membrane. Higher permeability lowers the membrane's unit capital cost by reducing the amount of membrane area required to treat a given volume of

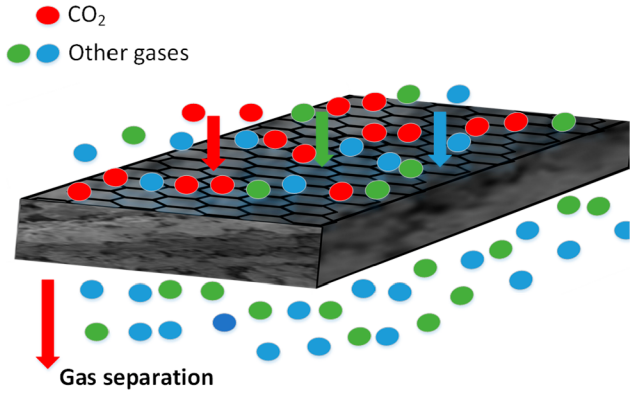

Figure 6. Mechanism of CO_2 separation in a graphene-based membrane.

https://doi.org/10.1021/acsomega.3c08722
ACS Omega 2024, 9, 20658−20669

Table 2. Information on the Performance and Conditions of Each Graphene-Based Membrane for Separating CO_2

graphene-composites	CO_2 permeability (barrers)	CO_2 permeance (GPU)	CO_2/N_2 selectivity	pressure (bar)	temperature (°C)	ref
GO-EDA membranes		660			75	35
PVAm-LG + 3% GO	71		59			42
PANI (2 wt %)/H-GO (1 wt %)	679		8.87	3	80	48
Pebax 2533/0.02% PGO	397		23.75			43
PIL-IL/GO		3090		1	22	39

gas. On the other hand, higher selectivity leads to purer gas products.[50−52]

Membrane technology is highly advantageous for industrial processes due to its benefits, including easy scalability, low energy consumption, and simple operation.[53] The absence of phase change or chemical additives and its modular design make it a popular choice in various fields, including water treatment,[52] gas purification,[54] food processing,[55] pharmaceutical industry,[56] and environmental protection.[57]

Membrane gas separation in the CCS field has received a lot of attention in recent years. Gas selectivity varies depending on molecular size, membrane material affinity, and molecular weight.[58] The gas is pressurized and connected to the atmosphere or vacuum to achieve a high permeate flux to create a greater driving force. However, given that the membrane's thickness is only a few hundred nanometers to a few microns, it cannot withstand such pressure. To ensure adequate mechanical strength, the membrane is typically coated onto a thick porous substrate.[59] Large pores that permit the free flow of gas to penetrate the top layer are necessary for the supporting substrate to provide the lowest possible flow resistance. Cracking and peeling may happen if the pores are too large and the substrate's surface is too rough. It is possible to achieve a more seamless transition between the substrate and the membrane by using an interlayer with much smaller pores.[60]

F. Zhou et al.[35] measured membrane gas permeation measurements using a gas permeation system they designed in their laboratory. The hollow fiber membrane coating module, which has a 1.35 cm^2 membrane permeation area, was housed in the stainless-steel filtration cell. They adjusted the feed gases with different volume concentrations using a mass flow controller (MFC) and helium as a sweep gas to carry the membrane permeate gas for compositional analysis. They tested dry and wet conditions, saturating the gases by bubbling them through a humidifier before passing them through water trappers (empty bottles filled with glass beads) to remove liquid water before entering the hollow fiber membrane permeation module. They calibrated the gas flow rates on the feed and permeate sides with a bubble flow meter and adjusted the feed pressure with a pressure regulator. To prevent sweeping gas backflow, the feed pressure was kept low at 1 psi, and the permeate pressure was set at atmospheric pressure. For the feed side and the sweep side, they set the feed and swept gas flow rates to 80 and 20 sccm, respectively.

Introducing a mixed gas (15 vol % CO_2 and 85 vol % N_2) as the feed gas, the GO EDA (ethylenediamine) membrane exhibited lower permeance for both gases than the previous GO-piperazine membrane under dry conditions, with 780 GPU (CO_2) and 820 GPU (N_2) at room temperature. Under the same coating conditions, this was primarily caused by the thicker GO-EDA membrane layer, while the poly(ether sulfone) (PES) support's selectivity essentially remained unchanged. The GO EDA membrane showed a CO_2 permeance of 60 GPU and a CO_2 selectivity of 70 at room temperature under wet conditions, indicating that water molecules adsorbed in the nanochannels of the GO-EDA membrane produced significant resistance to N_2 transport but little resistance for CO_2 permeation. To assess the impact of temperature on the mixed gas separation capabilities of GO-EDA membranes, the permeation temperature was raised. While N_2 permeability only slightly increased from 0.9 to 1.2 GPU, CO_2 permeability increased exponentially from 60 GPU (25 °C) to 660 GPU (75 °C)[35] as shown in Table 2.

To evaluate the membrane performance, Y.-Y. Lee and B. Gurkan[39] utilized a stainless-steel permeation module to bond the membrane. A mass flow controller was used to adjust the flow rates of dry CO_2, anhydrous N_2, and water-saturated N_2 while also controlling the temperature of the module. Air (410 ppm of CO_2) and cabin air (2500 ppm of CO_2) with varying relative humidity levels were included in the simulated feed gases. The fixed flow rates for the constant CO_2/N_2 feed and helium sweeps were 150 and 10 cm^3/min, respectively. Atmospheric pressure was kept constant on both sides of the membrane. Using a gas chromatograph, the sweep carried the permeate gas for quantitative composition analysis.

The poly(ionic liquid)-ionic liquid/GO (PIL-IL/GO) membrane demonstrated potential for the selective removal of CO_2 from ambient air and cabin air. Due to the semisolid PES layer on the surface, the PES/PET (poly(ethylene terephthalate)) substrate produced an unexpected CO_2/N_2 selectivity of 8. After GONF (The GO layer deposited on PES/PET is referred to as GONF) deposition, CO_2 and N_2 permeability decreased, but the GONF layer's high gas permeability and low resistance were preserved. Under direct air capture (DAC) conditions, the PIL-IL/GO membrane displayed a CO_2 permeance of 3090 GPU and a CO_2/N_2 selectivity of 1180. Similar results under spacecraft cabin conditions were obtained with 620 GPU CO_2 permeance and 250 GPU CO_2/N_2 selectivity. The N_2 permeability was effectively suppressed, and the facilitated transport mechanism of PIL-IL/GO was confirmed at low CO_2 concentrations. While saturation of carrier reactive sites at high CO_2 concentrations led to a downward trend in CO_2 permeance, the promising results of PIL-IL/GO suggest potential for future applications.[39]

A semipermeable barrier is used in the membrane process to physically separate certain chemicals as described by R. Casadei et al.[42] The substances that can penetrate the barrier are accumulated in the permeate stream, while the others remain in the retentate stream. A barometric technique is used to monitor the pressure rise brought on by the permeating gas in a downstream volume that is calibrated and constant to determine the system's permeability. Before conducting each test, it is crucial to eliminate any absorbed volatile species by placing the membrane in a permeation cell under vacuum for the night. After equilibrating the membrane and the flow at the needed relative humidity, the permeation test is initiated by

https://doi.org/10.1021/acsomega.3c08722
ACS Omega 2024, 9, 20658−20669

exposing the humidified feed gas to the upstream side of the film The only substance that ultimately causes the pressure to rise downstream is the gas under test because water is in equilibrium on both sides of the membrane.

Based on the experimental data, polyvinylamine-high grade (PVAm-HG) has a permeability of 4.2 barrers (relative humidity (RH) = 56%) with no clear pattern observed. On the other hand, PVAm-LG (low grade) has a CO_2 permeability range of 16.5 barrers (RH = 63%) to 73.8 barrers (RH = 93%). Filling the same polymer with 3 wt % GO ranged from 1.7 barrers (RH = 53%) to 71.0 barrers at high humidity. A PVAm-HG loaded with the same amount of GO, however, showed carbon dioxide permeabilities of 1.6 barrers (RH = 75%) and 25.1 barrers (RH = 93%). The same matrix showed values from 2.0 barrers (RH = 77%) to 23.1 barrers (RH = 92%) when loaded with multiple layers of graphene.[42]

According to the analysis of PVAm-LG and HG reinforced with GO, the low-grade polymer had a lower CO_2 selectivity of about 60 and a higher maximum CO_2 permeability of about 70 barrers when compared to the high-grade polymer. Compared to the former, the latter had a lower permeability of 35 barrers and a higher selectivity of about 80. This variation could be brought on by the two composite materials' various swelling patterns, as was previously mentioned. According to this, PVAm-LG + 3% GO is more hydrophilic than PVAm-HG based composites. When the humidity was increased from 60% to 95%, it was found that the selectivity for PVAm-LG + GO varied from 3.1 to 59.2. In contrast, for PVAm-HG, this amount ranged for the GO sample from 3.0 (RH = 75%) to 80.7 (RH = 95%) and for the graphene sample from 1.1 (RH = 82%) to 45.2 (RH = 95%).[42]

Experiments conducted by R. Casadei et al.[43] at 35 °C showed that adding graphene oxide substantially decreases the permeability for CO_2 and N_2. The Pebax-based mixed matrix membranes (MMM) showed decreasing permeabilities with each increase in the percentage of GO, leading to notable drops in CO_2 and nitrogen from 365 to 51 barrers and 15 to 2 barrers, respectively. In the composites with lower loading, there was only a very slight increase in CO_2 permeability (371 barrers compared to 365 barrers measured for pure Pebax), indicating that the observed trend was only an exception in these composites. The reactions of various GO-based fillers, such as PEAGO (GO functionalized with polyetheramine) and PGO (porous graphene oxide), were tested in Pebax 2533 membranes blended with a loading of 0.02% by weight. PEAGO and PGO both marginally enhanced the permselective properties, with differences ranging from 4% to 8% (higher than the acknowledged experimental error). When PEAGO was added to the sample, the CO_2 permeability increased to 380 barrers, and when PGO was added to the Pebax, it increased even more to 397 barrers. Hence, it is evident that GO-based fillers can significantly enhance the permselective properties of Pebax membranes.

A study on pure gas permeability was carried out by H. Kweon et al.[48] at room temperature using the conventional constant/variable pressure method. Additionally, they examined the ideal selectivity (CO_2/N_2) and pure CO_2 and N_2 permeabilities of PANI and GO/PANI membranes based on their composition (GO:PANI ratio) at a feed pressure of 0.30 MPa. The CO_2 permeability and CO_2/N_2 selectivity of PANI membranes ranged from 172 to 208 barrers and 3.63 to 3.69, respectively. The packing of the PANI polymer chains is thought to be disrupted by the addition of GO, increasing the free volume as a result. Additionally, increased gas diffusion occurs within the GO/PANI membrane as a result of the oxidized regions on the basal plane creating channels for gas molecules to pass through.

Selectivity ought to decline while permeability ought to rise as free volume rises. However, given that individual GO sheets are only marginally thicker than CO_2 and N_2 gas molecules, the effect of increasing free volume on selectivity may not be significant. Instead, the artificially generated internal layer can trap gas molecules. Therefore, the composite membrane with GO may exhibit higher gas permeability capability but comparable or slightly lower gas selectivity than the membrane without GO if the number of functional groups in the GO layer is controlled. The CO_2 permeability of 679 barrers and a CO_2/N_2 selectivity of 4.41, which are greater than those of the pure PANI membrane, are produced by the mixture of 2 wt % PANI + 1 wt % H-GO (highly oxidized GO) in NMP solvent.[48]

Photocatalytic Reduction. Photocatalytic reduction operates through an oxidation−reduction process that utilizes photoenergy.[61] This process is analogous to photosynthesis and involves two fundamental steps: the absorption of CO_2 by photocatalytic materials, followed by conversion, and the reaction between CO_2 and photogenerated electron holes. The amount of light energy necessary for a photocatalytic reaction depends on the photocatalyst's valence band and conduction band, as well as the excitation and separation energies of electron−hole pairs.[62] When exposed to light with an energy level that is equal to or higher than the band gap, electrons in the photocatalyst crystal will either be excited or move from the valence band to the conduction band, leaving holes in the valence band. Depending on the difference in reduction potential and the quantity of transferred electrons, photogenerated electrons exhibit strong reduction ability in the presence of H_2O. Hydrocarbons like HCHO, HCOOH, CH_3OH, and CH_4 are subsequently formed from the reduction of CO_2. Instead, because they can pick up electrons and release O_2, photogenerated holes exhibit strong oxidizing properties.[63,64]

Figure 7 depicts the photocatalytic conversion of CO_2 using transition metal oxides, which are the most frequently used catalysts. The photocatalytic process was tested by A. W. Morawski et al.[37] using a batch-mixed photoreactor. An 8 W Hg lamp (254 nm) was utilized as the irradiation source, placed above a quartz glass window in the photoreactor cover.

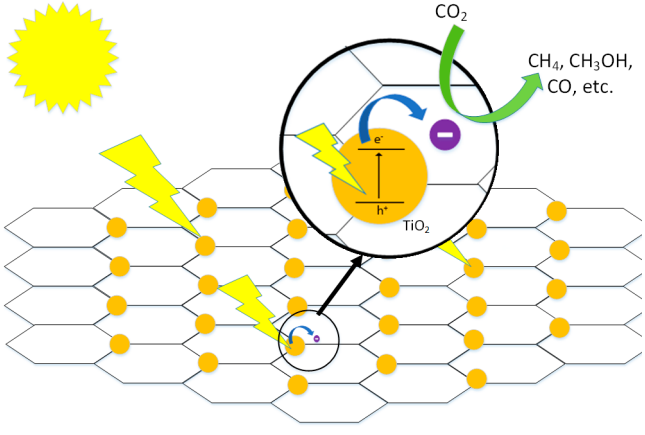

Figure 7. Mechanism converts CO_2 to other gases by photocatalytic conversion.

https://doi.org/10.1021/acsomega.3c08722
ACS Omega 2024, 9, 20658−20669

Gas chromatography equipped with a BID (barrier discharge ionization detector) was used to analyze each gas sample. To collect samples for analysis, the reaction mixture was exposed to radiation for time intervals ranging from 0 to 8 h. Each measurement was carried out in a repeatable manner.

Hydrogen was present during the process, which turned CO_2 into methane and carbon monoxide. In the presence of TiO_2/rGO photocatalyst and reference materials, the study concentrated on the impact of irradiation time (0−8 h) on the formation of gaseous products. In comparison to the initial TiO_2, only two samples, TiO_2/rGO-10 (10% represents the weight of the rGO mass) and TiO_2/rGO-10-500 (500 °C represents the calcination temperature), had higher yields of all products. Generally, the TiO_2/rGO-10 material demonstrated the highest activity in all situations. The CH_4, CO_2, and H_2 yields for this substance were 15.87, 2.98, and 113 mol/photocatalyst after 8 h of radiation, respectively. Notably, the photocatalytic performance of CO_2 reduction was significantly enhanced by the modification of rGO.[37] In their study, L. Wang et al.[38] found that ZnO/graphene has a higher CO_2 absorption capacity (0.021 mmol/g) compared to ZnO (0.015 mmol/g) due to the $\pi-\pi$-conjugation interaction between graphene and CO_2 molecules. The photocatalytic CO_2 reduction (PCR) activity was evaluated under simulated solar light irradiation, with CO, CH_3OH, and CH_4 identified as the main reduction products.

ZnO exhibited evolution rates of 1.26 μmol/h for CO and 0.31 μmol/h for CH_3OH, with trace amounts of CH_4 also detected. The evolution rates of these three reduction products, however, significantly increased when the loading amount of graphene was 0.4% (0.5 mL of benzene, ZnO/graphene), reaching values as high as 3.38, 0.59, and 0.09 mol/h, respectively. It is significant to note that the PCR results of the samples (ZnO/0.8%graphene and ZnO/1%graphene) degraded with increasing graphene content, which may be related to the excessive shielding effect of graphene. Nevertheless, regardless of the loading content of graphene, the evolution rate of each product obtained via ZnO/graphene is higher than that of ZnO. The samples also contained the primary oxidation product, O_2, with ZnO/graphene having a higher yield rate than ZnO.[38]

CONCLUSION AND PERSPECTIVE

CO_2 released by human activities like burning fossil fuels and deforestation is more than can be absorbed by natural processes.[65] As a result, the amount of CO_2 in the atmosphere rises and causes more severe weather conditions. Carbon capture and storage (CCS) is a method to reduce CO_2 emissions, and graphene-based materials are being studied for their potential in applications such as CO_2 separation. Graphene is a material renowned for its exceptional physical and chemical properties, but producing it on a large scale is a challenging task. Fortunately, derivatives of graphene such as GO and rGO can be produced on a larger scale. Depending on the level of oxidation and the precise surface area of the smaller GO sheet, GO has a low electrical conductivity and behaves in an insulating or semiconductive manner. Although the reduction of GO is a promising method for obtaining graphene-like properties, rGO still contains oxygen residues and structural flaws from the chemical oxidation synthesis of GO, making the creation of a pure graphene structure impossible.[66] The reduction process significantly modifies the GO's mechanical strength, stability, dispersibility, reactivity, and structural characteristics. The removal of oxygen-containing compounds from the GO structure and restoration of the sp^2 structure following the reduction process is to blame for this modification.[67]

A comprehensive review of CO_2 reduction by graphene is urgently needed. Graphene-based composites have been studied extensively, with derivatives such as GO and rGO being prepared through various methods. GO can be obtained through the Hummer method or by adding L-ascorbic acid or L-arginine to the GO dispersion. The rGO can be synthesized through thermal, solvothermal, or hydrothermal reduction. Other modified GO includes UV-GO, P-GO, and H-GO. Porous graphene oxide (PGO) can be synthesized by sonicating a GO dispersion with NH_4OH and H_2O_2.

This Review thoroughly examines the latest breakthroughs in carbon capture, specifically graphene's efficacy in separating CO_2. It serves as a foundation for future research by merging graphene composite separation technology, a highly efficient substitute, with the currently booming use of graphene material in various applications. The application of graphene in reducing CO_2 concentration was investigated by different methods, namely adsorption, membrane separation, and photocatalytic reduction. These three methods are the best methods in carbon capture applications. Adsorption and photocatalytic methods calculated decreasing CO_2 concentration, while the membrane method reported CO_2 permeability and selectivity of CO_2/CH_4 and CO_2/N_2.

Adsorption methods typically use materials with high porosity for better CO_2 adsorption, but the saturation limits the adsorption process. The main challenge is to increase the surface area and volume of micropores which can enhance CO_2 adsorption capacity.[40] Graphene-based material with large surface area is suitable for those purposes; therefore, it can improve its capacity in CO_2 adsorption. Photocatalysts usually use semiconductor materials that can be active when illuminated by photoenergy. Semiconductors will release electron−hole pairs that will react with CO_2 to form new energy such as CH_4, CH_3OH, CO, etc. However, semiconductors usually do not have good conductivity so compositing with graphene which has great conductivity will improve its performance. Graphene-based membranes have high strength and are resistant to pressure and stress. In membrane separation, graphene has high molecular selectivity to CO_2. In addition, the thin graphene structure gives the membrane a high permeability capability. Therefore, graphene membranes can provide good CO_2 permeation rates.[68]

Among the three methods for measuring CO_2 separation that were reviewed from 15 journals, there are promising results. In the CO_2 adsorption measurements, the rGO/$ACNF_{0.1}$ shows the best adsorption which was 58 mmol/g.[45] In gas permeation measurements, there are two different outputs: CO_2 permeability and CO_2 permeation. At CO_2 permeability output, PANI (2 wt %)/H-GO (1 wt %) shows the best result with 679 barrers, but the selectivity is very low.[48] Good selectivity is PVAm-LG + 3% GO, but the permeability is low.[42] For output CO_2 permeation, the best is PIL-IL/GO with 3090 GPU,[39] and the last is photocatalytic reduction measurement with the best result being ZnO/graphene with 0.021 mmol/g.[38]

In carbon capture, parameters such as temperature, flow rate, humidity, and pressure play important roles in adsorption, photocatalytic, and membrane methods. Proper temperature selection greatly affects CO_2 reduction results. Previous

https://doi.org/10.1021/acsomega.3c08722
ACS Omega 2024, 9, 20658−20669

research states that a temperature of 50 °C has more adsorption results than temperatures of 25 and 100 °C.[34] Other studies also mention the activation temperature at 600 °C is better than that at 400, 500, and 700 °C.[41]

At lower flow rates, CO_2 gas particles have more time to interact with the adsorbent surface and diffuse through the adsorbent pores.[34] This diffusion allows the gas molecules to better penetrate the adsorbent pore structure and bond to the adsorbent surface. Thus, the use of lower flow rates may match the optimal conditions for CO_2 adsorption. At higher humidity, CO_2 adsorption is better. This is because water molecules (H_2O) can react with CO_2 to form carbonic acid (H_2CO_3). This reaction can increase CO_2 adsorption ability due to additional interactions between carbonic acid and adsorbent.[69]

At low pressures, there is high CO_2 absorption because CO_2 gas molecules interact with the surface of solids chemically, thus forming chemical bonds with graphene and its composite materials. However, at higher pressures, the increase in CO_2 capacity slows down; this is attributed to the presence of physical adsorption where CO_2 molecules adhere to the surface of solids without forming strong chemical bonds.[40]

From the results of the review we found that many things can be developed for carbon capture applications. So far, as shown in Figure 1 that low cost is one of the criteria in selection adsorbent, the challenge is that the costs incurred are large but the results obtained are very small so that it is not effective (as in the conversion obtained only of the micro order). By functionalized graphene and combining it with other materials, it is expected to produce a low-cost material that can effectively reduce CO_2 emissions. This Review highlights the opportunities in modifying graphene with other materials, as well as the need for more effective methods. Recently, there has been a lot of attention on graphene material composited with amines, but there are still only a few studies on it. Therefore, with a proper modification, this material has the potential to be an effective material for CO_2 separation.

AUTHOR INFORMATION

Corresponding Author

Fitrilawati − *Department of Physics, Faculty of Mathematics and Natural Sciences, Padjadjaran University, Sumedang 45363, Indonesia*; Email: fitrilawati@unpad.ac.id

Authors

Tri Komala Junita − *Department of Physics, Faculty of Mathematics and Natural Sciences, Padjadjaran University, Sumedang 45363, Indonesia; Department of Biotechnology, Faculty of Graduate School, Padjadjaran University, Bandung 40132, Indonesia;* orcid.org/0009-0007-9152-2865

Norman Syakir − *Department of Physics, Faculty of Mathematics and Natural Sciences, Padjadjaran University, Sumedang 45363, Indonesia*

Ferry Faizal − *Department of Physics, Faculty of Mathematics and Natural Sciences, Padjadjaran University, Sumedang 45363, Indonesia*

Complete contact information is available at: https://pubs.acs.org/10.1021/acsomega.3c08722

Author Contributions

T.K.J.: writing—original draft, visualization, and conceptualization. F.F.: supervision and conceptualization. N.S.: review and investigation. F.: supervision, writing—review, and editing.

Notes

The authors declare no competing financial interest.

ACKNOWLEDGMENTS

This research was funded by the Padjadjaran University, Indonesia, through the research grant scheme of Padjadjaran Scholarship for Graduate Program (BUPP), contract number 1549/UN6.3.1/PT.00/2023, dated on March 27, 2023.

REFERENCES

(1) Atmospheric CO_2. August 2023. https://www.co2.earth (accessed August 9, 2023).

(2) Stein, T. Carbon dioxide now more than 50% higher than pre-industrial levels. https://www.noaa.gov/news-release/carbon-dioxide-now-more-than-50-higher-than-pre-industrial-levels (accessed February 9, 2023).

(3) Kang, M. J.; Kim, C. W.; Cha, H. G.; Pawar, A. U.; Kang, Y. S. Selective liquid chemicals on CO2 reduction by energy level tuned rGO/TiO2 dark cathode with BiVO4 photoanode. *Appl. Catal. B: Environmental* **2021**, *295*, 120267.

(4) Abuelnoor, N.; AlHajaj, A.; Khaleel, M.; Vega, L. F.; Abu-Zahra, M. R. M. Activated carbons from biomass-based sources for CO(2) capture applications. *Chemosphere* **2021**, *282*, 131111.

(5) Al Mesfer, M. K.; Danish, M.; Fahmy, Y. M.; Rashid, M. M. Post-combustion CO2 capture with activated carbons using fixed bed adsorption. *Heat and Mass Transfer* **2018**, *54* (9), 2715−2724.

(6) Cui, Z.; deMontigny, D. Part 7: A review of CO2capture using hollow fiber membrane contactors. *Carbon Management* **2013**, *4* (1), 69−89.

(7) Salvinder, K. M. S.; Zabiri, H.; Taqvi, S. A.; Ramasamy, M.; Isa, F.; Rozali, N. E. M.; Suleman, H.; Maulud, A.; Shariff, A. M. An overview on control strategies for CO2 capture using absorption/stripping system. *Chem. Eng. Res. Des.* **2019**, *147*, 319−337.

(8) Yousef, A. M.; El-Maghlany, W. M.; Eldrainy, Y. A.; Attia, A. New approach for biogas purification using cryogenic separation and distillation process for CO2 capture. *Energy* **2018**, *156*, 328−351.

(9) Güleç, F.; Meredith, W.; Sun, C.-G.; Snape, C. E. A novel approach to CO2 capture in Fluid Catalytic Cracking—Chemical Looping Combustion. *Fuel* **2019**, *244*, 140−150.

(10) Tan, T. A.; Yusuf, S. Y.; Fazara, M. Electrochemical reduction of carbon dioxide into formate. *J. Eng. Sci. Technol.* **2015**, *10*, 23−29.

(11) Shi, H.; Naami, A.; Idem, R.; Tontiwachwuthikul, P. Catalytic and non catalytic solvent regeneration during absorption-based CO2 capture with single and blended reactive amine solvents. *International Journal of Greenhouse Gas Control* **2014**, *26*, 39−50.

(12) Lum, Y.; Yue, B.; Lobaccaro, P.; Bell, A. T.; Ager, J. W. Optimizing C−C Coupling on Oxide-Derived Copper Catalysts for Electrochemical CO2 Reduction. *J. Phys. Chem. C* **2017**, *121* (26), 14191−14203.

(13) Gao, J.; Jia, C.; Liu, B. Direct and selective hydrogenation of CO2 to ethylene and propene by bifunctional catalysts. *Catalysis Science & Technology* **2017**, *7* (23), 5602−5607.

(14) Bafaqeer, A.; Tahir, M.; Amin, N. A. S. Synthesis of hierarchical ZnV2O6 nanosheets with enhanced activity and stability for visible light driven CO2 reduction to solar fuels. *Appl. Surf. Sci.* **2018**, *435*, 953−962.

(15) de Richter, R. K.; Ming, T.; Caillol, S. Fighting global warming by photocatalytic reduction of CO2 using giant photocatalytic reactors. *Renew. Sustain. Energy Rev.* **2013**, *19*, 82−106.

(16) Stanton Ribeiro, M.; Zanatta, M.; Corvo, M. C. Ionic liquids and biomass as carbon precursors: Synergistically answering a call for CO2 capture and conversion. *Fuel* **2022**, *327*, 125164.

(17) Cheung, O.; Bacsik, Z. n.; Fil, N.; Krokidas, P.; Wardecki, D.; Hedin, N. Selective Adsorption of CO2 on Zeolites NaK-ZK-4 with Si/Al of 1.8−2.8. *ACS omega* **2020**, *5* (39), 25371−25380.
(18) Khdary, N. H.; Alayyar, A. S.; Alsarhan, L. M.; Alshihri, S.; Mokhtar, M. Metal Oxides as Catalyst/Supporter for CO2 Capture and Conversion Review. *Catalysts* **2022**, *12* (3), 300.
(19) Lu, W.; Sculley, J. P.; Yuan, D.; Krishna, R.; Zhou, H.-C. Carbon Dioxide Capture from Air Using Amine-Grafted Porous Polymer Networks. *J. Phys. Chem. C* **2013**, *117* (8), 4057−4061.
(20) Aniruddha, R.; Sreedhar, I.; Reddy, B. M. MOFs in carbon capture-past, present and future. *J. CO_2 Util.* **2020**, *42*, 101297.
(21) Zhao, P.; Zhang, G.; Hao, L. A novel blended amine functionalized porous silica adsorbent for carbon dioxide capture. *Adsorption* **2020**, *26* (5), 749−764.
(22) Mehra, P.; Paul, A. Decoding Carbon-Based Materials' Properties for High CO2 Capture and Selectivity. *ACS Omega* **2022**, *7* (38), 34538−34546.
(23) Yadav, S.; Singh Raman, A. P.; Meena, H.; Goswami, A. G.; Bhawna; Kumar, V.; Jain, P.; Kumar, G.; Sagar, M.; Rana, D. K.; et al. An update on graphene oxide: applications and toxicity. *ACS Omega* **2022**, *7* (40), 35387−35445.
(24) Fitrilawati; Marcelina, V.; Dzujah, D. U.; Bahtiar, A.; Hartati, Y. W.; Syakir, N. Energy Storage Characteristics of Electrochemically Deposited Graphene Oxide on ITO and Cu Substrates. *Mater. Sci. Forum* **2019**, *966*, 428−432.
(25) Ju, J.; Zhang, R.; Chen, W. Photochemical deposition of surface-clean silver nanoparticles on nitrogen-doped graphene quantum dots for sensitive colorimetric detection of glutathione. *Sens. Actuators, B* **2016**, *228*, 66−73.
(26) Aurellia, J. M.; Maulida, G.; Dzujah, D. U.; Syakir, N.; Fitrilawati, F. Effect of Stirring Time on Methylene Blue Adsorption onto Graphene Oxides Surfaces. *Mater. Sci. Forum* **2021**, *1028*, 291−295.
(27) Marcelina, V.; Syakir, N.; Wyantuti, S.; Hartati, Y. W.; Hidayat, R.; Fitrilawati. Characteristic of thermally reduced graphene oxide as supercapacitors electrode materials. *IOP Conf. Ser.: Mater. Sci. Eng.* **2017**, *196*, 012034.
(28) Gong, L.; Young, R. J.; Kinloch, I. A.; Riaz, I.; Jalil, R.; Novoselov, K. S. Optimizing the reinforcement of polymer-based nanocomposites by graphene. *ACS Nano* **2012**, *6* (3), 2086−2095.
(29) Singh, S.; Varghese, A. M.; Reinalda, D.; Karanikolos, G. N. Graphene-based membranes for carbon dioxide separation. *J. CO_2 Util.* **2021**, *49*, 101544.
(30) Garrafa-Gálvez, H. E.; Alvarado-Beltrán, C. G.; Almaral-Sánchez, J. L.; Hurtado-Macías, A.; Garzon-Fontecha, A. M.; Luque, P. A.; Castro-Beltrán, A. Graphene role in improved solar photocatalytic performance of TiO2-RGO nanocomposite. *Chem. Phys.* **2019**, *521*, 35−43.
(31) Hack, J.; Maeda, N.; Meier, D. M. Review on CO2 capture using amine-functionalized materials. *ACS omega* **2022**, *7* (44), 39520−39530.
(32) Yoo, B. M.; Shin, J. E.; Lee, H. D.; Park, H. B. Graphene and graphene oxide membranes for gas separation applications. *Current Opinion in Chemical Engineering* **2017**, *16*, 39−47.
(33) Khandaker, T.; Hossain, M. S.; Dhar, P. K.; Rahman, M. S.; Hossain, M. A.; Ahmed, M. B. Efficacies of Carbon-Based Adsorbents for Carbon Dioxide Capture. *Processes* **2020**, *8* (6), 654.
(34) Zhao, Y.; Ge, H.; Miao, Y.; Chen, J.; Cai, W. CO2 capture ability of Cu-based metal-organic frameworks synergized with amino acid-functionalized layered materials. *Catal. Today* **2020**, *356*, 604−612.
(35) Zhou, F.; Tien, H. N.; Dong, Q.; Xu, W. L.; Li, H.; Li, S.; Yu, M. Ultrathin, ethylenediamine-functionalized graphene oxide membranes on hollow fibers for CO2 capture. *J. Membr. Sci.* **2019**, *573*, 184−191.
(36) Yang, Y.; Liu, M.; Han, S.; Xi, H.; Xu, C.; Yuan, R.; Long, J.; Li, Z. Double-sided modification of TiO2 spherical shell by graphene sheets with enhanced photocatalytic activity for CO2 reduction. *Appl. Surf. Sci.* **2021**, *537*, 147991.
(37) Morawski, A.; Kusiak-Nejman, E.; Wanag, A.; Narkiewicz, U.; Edelmannová, M.; Reli, M.; Kočí, K. Influence of the calcination of TiO2-reduced graphite hybrid for the photocatalytic reduction of carbon dioxide. *Catal. Today* **2021**, *380*, 32−40.
(38) Wang, L.; Tan, H.; Zhang, L.; Cheng, B.; Yu, J. In-situ growth of few-layer graphene on ZnO with intimate interfacial contact for enhanced photocatalytic CO2 reduction activity. *Chem. Eng. J.* **2021**, *411*, 128501.
(39) Lee, Y.-Y.; Gurkan, B. Graphene oxide reinforced facilitated transport membrane with poly (ionic liquid) and ionic liquid carriers for CO2/N2 separation. *J. Membr. Sci.* **2021**, *638*, 119652.
(40) Wang, Y.; Wang, H.; Zhang, T. C.; Yuan, S.; Liang, B. N-doped porous carbon derived from rGO-Incorporated polyphenylenediamine composites for CO2 adsorption and supercapacitors. *J. Power Sources* **2020**, *472*, 228610.
(41) Xiao, J.; Wang, Y.; Zhang, T. C.; Yuan, S. rGO/N-porous carbon composites for enhanced CO2 capture and energy storage performances. *J. Alloys Compd.* **2021**, *857*, 157534.
(42) Casadei, R.; Venturi, D.; Giacinti Baschetti, M.; Giorgini, L.; Maccaferri, E.; Ligi, S. Polyvinylamine Membranes Containing Graphene-Based Nanofillers for Carbon Capture Applications. *Membranes (Basel)* **2019**, *9* (9), 119.
(43) Casadei, R.; Giacinti Baschetti, M.; Yoo, M. J.; Park, H. B.; Giorgini, L. Pebax((R)) 2533/Graphene Oxide Nanocomposite Membranes for Carbon Capture. *Membranes (Basel)* **2020**, *10* (8), 188.
(44) Ouyang, L.; Xiao, J.; Jiang, H.; Yuan, S. Nitrogen-Doped Porous Carbon Materials Derived from Graphene Oxide/Melamine Resin Composites for CO(2) Adsorption. *Molecules* **2021**, *26* (17), 5293.
(45) Che Othman, F. E.; Yusof, N.; Gonzalez-Benito, J.; Fan, X.; Ismail, A. F. Electrospun Composites Made of Reduced Graphene Oxide and Polyacrylonitrile-Based Activated Carbon Nanofibers (rGO/ACNF) for Enhanced CO(2) Adsorption. *Polymers (Basel)* **2020**, *12* (9), 2117.
(46) Ren, W.; Wei, Z.; Xia, X.; Hong, Z.; Li, S. CO_2 adsorption performance of CuBTC/graphene aerogel composites. *J. Nanopart. Res.* **2020**, *22* (7)..
(47) Varghese, A. M.; Reddy, K. S. K.; Bhoria, N.; Singh, S.; Pokhrel, J.; Karanikolos, G. N. Enhancing effect of UV activation of graphene oxide on carbon capture performance of metal-organic framework/graphene oxide hybrid adsorbents. *Chem. Eng. J.* **2021**, *420*, 129677.
(48) Kweon, H.; Lin, C.-W.; Faruque Hasan, M. M.; Kaner, R.; Sant, G. N. Highly Permeable Polyaniline−Graphene Oxide Nanocomposite Membranes for CO2 Separations. *ACS Appl. Polym. Mater.* **2019**, *1* (12), 3233−3241.
(49) Page, M. J.; McKenzie, J. E.; Bossuyt, P. M.; Boutron, I.; Hoffmann, T. C.; Mulrow, C. D.; Shamseer, L.; Tetzlaff, J. M.; Akl, E. A.; Brennan, S. E.; et al. The PRISMA 2020 statement: an updated guideline for reporting systematic reviews. *Int. J. Surgery* **2021**, *88*, 105906.
(50) Muthukumaraswamy Rangaraj, V.; Wahab, M. A.; Reddy, K. S. K.; Kakosimos, G.; Abdalla, O.; Favvas, E. P.; Reinalda, D.; Geuzebroek, F.; Abdala, A.; Karanikolos, G. N. Metal Organic Framework - Based Mixed Matrix Membranes for Carbon Dioxide Separation: Recent Advances and Future Directions. *Front Chem.* **2020**, *8*, 534.
(51) Robeson, L. M. The upper bound revisited. *J. Membr. Sci.* **2008**, *320* (1−2), 390−400.
(52) Maier, G. Gas separation with polymer membranes. *Angew. Chem., Int. Ed.* **1998**, *37* (21), 2960−2974.
(53) Othman, N. H.; Alias, N. H.; Fuzil, N. S.; Marpani, F.; Shahruddin, M. Z.; Chew, C. M.; David Ng, K. M.; Lau, W. J.; Ismail, A. F. A Review on the Use of Membrane Technology Systems in Developing Countries. *Membranes* **2022**, *12* (1), 30.
(54) Zhang, Y.; Sunarso, J.; Liu, S.; Wang, R. Current status and development of membranes for CO2/CH4 separation: A review. *International Journal of Greenhouse Gas Control* **2013**, *12*, 84−107.

https://doi.org/10.1021/acsomega.3c08722
ACS Omega 2024, 9, 20658−20669

(55) Charcosset, C. Preparation of emulsions and particles by membrane emulsification for the food processing industry. *J. Food Eng.* **2009**, *92* (3), 241−249.
(56) Zaviska, F.; Drogui, P.; Grasmick, A.; Azais, A.; Héran, M. Nanofiltration membrane bioreactor for removing pharmaceutical compounds. *J. Membr. Sci.* **2013**, *429*, 121−129.
(57) Ambashta, R. D.; Sillanpaa, M. E. Membrane purification in radioactive waste management: a short review. *J. Environ. Radioact* **2012**, *105*, 76−84.
(58) Liu, S. L.; Shao, L.; Chua, M. L.; Lau, C. H.; Wang, H.; Quan, S. Recent progress in the design of advanced PEO-containing membranes for CO2 removal. *Prog. Polym. Sci.* **2013**, *38* (7), 1089−1120.
(59) Simon, C.; Endres, J.; Nefzger-Loders, B.; Wilhelm, F.; Gasteiger, H. A. Interaction of Pore Size and Hydrophobicity/Hydrophilicity for Improved Oxygen and Water Transport through Microporous Layers. *J. Electrochem. Soc.* **2019**, *166* (13), F1022−F1035.
(60) Ji, G.; Zhao, M. Membrane Separation Technology in Carbon Capture. In *Recent Advances in Carbon Capture and Storage*; IntechOpen Ltd.: London, 2017.
(61) Rehman, Z. U.; Bilal, M.; Hou, J.; Butt, F. K.; Ahmad, J.; Ali, S.; Hussain, A. Photocatalytic CO(2) Reduction Using TiO(2)-Based Photocatalysts and TiO(2) Z-Scheme Heterojunction Composites: A Review. *Molecules* **2022**, *27* (7), 2069.
(62) Shehzad, N.; Tahir, M.; Johari, K.; Murugesan, T.; Hussain, M. Improved interfacial bonding of graphene-TiO2 with enhanced photocatalytic reduction of CO2 into solar fuel. *Journal of Environmental Chemical Engineering* **2018**, *6* (6), 6947−6957.
(63) Rodríguez, V.; Camarillo, R.; Martínez, F.; Jiménez, C.; Rincón, J. High-pressure synthesis of rGO/TiO2 and rGO/TiO2/Cu catalysts for efficient CO2 reduction under solar light. *J. Supercrit. Fluids* **2021**, *174*, 105265.
(64) Ohtani, B. Photocatalysis A to Z—What we know and what we do not know in a scientific sense. *Journal of Photochemistry and Photobiology C: Photochemistry Reviews* **2010**, *11* (4), 157−178.
(65) The Causes of Climate Change. https://climate.nasa.gov/causes/ (accessed September 21, 2023).
(66) Shen, J.; Yan, B.; Shi, M.; Ma, H.; Li, N.; Ye, M. One step hydrothermal synthesis of TiO2-reduced graphene oxide sheets. *J. Mater. Chem.* **2011**, *21* (10), 3415.
(67) Zhang, Q.; Lin, C. F.; Jing, Y. H.; Chang, C. T. Photocatalytic reduction of carbon dioxide to methanol and formic acid by graphene-TiO2. *J. Air Waste Manag Assoc* **2014**, *64* (5), 578−85.
(68) Ali, A.; Pothu, R.; Siyal, S. H.; Phulpoto, S.; Sajjad, M.; Thebo, K. H. Graphene-based membranes for CO2 separation. *Materials Science for Energy Technologies* **2019**, *2* (1), 83−88.
(69) Taifan, W.; Boily, J.-F.; Baltrusaitis, J. Surface chemistry of carbon dioxide revisited. *Surf. Sci. Rep.* **2016**, *71* (4), 595−671.

https://doi.org/10.1021/acsomega.3c08722
ACS Omega 2024, 9, 20658−20669